

REPORT
OF
OCCO
A

JOHN

HIS

MEN

RE

IBI

Los Alamos National Laboratory is operated by the University of California for the United States Department of Energy under contract W-7405-ENG-36

LA-UR--82-1156

PLS 013950

TITLE: NUMERICAL SIMULATION OF FRACTURE

AUTHOR(S): L. G. Margolin and T. F. Adams

SUBMITTED TO: 23rd Symposium on Rock Mechanics, University of California,
Berkeley, CA, August 25-27, 1982

MASTER

By acceptance of this article, the publisher recognizes that the U.S. Government retains a nonexclusive, royalty-free license to publish or reproduce the published form of this contribution or to allow others to do so, for U.S. Government purposes.

The Los Alamos National Laboratory requests that the publisher identify this article as work performed under the auspices of the U.S. Department of Energy.

Los Alamos Los Alamos National Laboratory
Los Alamos, New Mexico 87545

NUMERICAL SIMULATION OF FRACTURE

by L. G. Margolin and T. F. Adams

Earth and Space Science Division
Los Alamos National Laboratory
Los Alamos, New Mexico

ABSTRACT

The Bedded Crack Model (BCM) is a constitutive model for brittle materials. It is based on effective modulus theory and makes use of a generalized Griffith criterion for crack growth. It is used in a solid dynamic computer code to simulate stress wave propagation and fracture in rock. A general description of the model is given and then the theoretical basis for it is presented. Some effects of finite cell size in numerical simulations are discussed. The use of the BCM is illustrated in simulations of explosive fracture of oil shale. There is generally good agreement between the calculations and data from field experiments.

INTRODUCTION

Numerical simulation of stress wave propagation and fracture in rock is a topic of great current interest and importance. Applications of numerical programs range from in situ techniques for recovery of energy and mineral resources to nuclear weapons testing, and even to the study of earthquakes.

Numerical simulation requires a solid dynamic computer code to simulate stress wave propagation and a constitutive model to represent the material response, including fracture. The Bedded Crack Model (BCM) is a constitutive model that has been developed for brittle materials. It is based on a microphysical picture in which the evolution of a statistical distribution of penny shaped cracks is calculated.

The BCM addresses two questions. For a material containing penny shaped cracks:

- 1) how does the stress field affect the cracks - that is, when can cracks grow?

- 2) how do the cracks affect the material properties - that is, what are the effective elastic moduli of a cracked material?

Intrinsic to the model is the statistical framework used to describe the distribution of cracks as a function of size.

In the next section, we describe the theoretical basis of the model. We then investigate some effects of finite cell size in numerical simulation of stress wave propagation. Finally, we illustrate the use of the BCM in a stress wave code to simulate blasting in oil shale. In general, the calculations agree with data from field experiments.

THEORETICAL BASIS

Griffith Criterion

The question of when a crack can grow is answered by a generalized Griffith criterion. The criterion says that a crack will grow whenever that growth reduces the potential energy of the crack and the material that contains it. Griffith (1920) applied this criterion to the case of a two-dimensional crack (slit) in normal tension. We have generalized Griffith's analysis to three-dimensional (penny shaped) cracks in the x-y plane. A crack of radius c in normal tension will grow if

$$\sigma_{zz}^2 + \left(\frac{2}{2-\nu}\right) (\sigma_{xz}^2 + \sigma_{yz}^2) \geq \frac{4\pi TE}{c} \quad (1)$$

Here ν is Poisson's ratio, E is Young's modulus and T is the surface tension. Equation 1 shows that in a given stress field, there is a critical crack size. Cracks bigger than the critical size grow, while smaller cracks are stable. The equation also shows that the effect of shear stress is to reduce the critical crack size.

The criterion can also be applied to closed cracks (normal compression). In this case, friction between the crack faces becomes important (McClintock and Walsh, 1962). The criterion for closed cracks has the form

$$\left(\frac{2}{2-\nu}\right) \left[\sigma_{xz}^2 + \sigma_{yz}^2 - (\tau_c - \mu \sigma_{zz})^2 \right] \geq \frac{4\pi TE}{c} \quad (2)$$

Here μ is the dynamic coefficient of friction and τ_c represents a cohesion.

Effective Elastic Moduli

The effective moduli are found from static solutions for strain as a function of applied stress in a randomly cracked body.

The basic assumption is that the total strain can be written as the sum of the strain in the material of the body plus the additional strain due to opening and sliding of the cracks. The additional strain due to the cracks is linear in the applied stress if crack interactions are ignored (Hoenig, 1979). Thus we can write

$$\epsilon_{ij} = (M_{ijkl} + \tilde{M}_{ijkl}) \sigma_{kl} \quad (3)$$

Here M_{ijkl} is the modulus of the uncracked material. \tilde{M}_{ijkl} is proportional to the third moment of the crack distribution.

The crack size distribution changes with time as the cracks grow. The constitutive law then is

$$\frac{d\sigma_{kl}}{dt} = C_{ijkl} \left(\frac{d\epsilon_{ij}}{dt} - \frac{d\tilde{M}_{ijmn}}{dt} \right) \sigma_{mn} \quad (4)$$

where $C = (M + \tilde{M})^{-1}$. Thus, the constitutive relation has the form of a Maxwell solid with a variable relaxation time.

Crack Statistics

The initial distribution of cracks is assumed to be exponential: the number of cracks with radius greater than c is $N_0 \exp(-c/\bar{c})$. The constant \bar{c} is a characteristic length scale of the initial distribution and N_0 is the total number of cracks per unit volume. The exponential dependence is not crucial to the model, but is convenient and is consistent with data for many rocks (Shockey et al., 1974).

At the beginning of each computational cycle, we use the Griffith criterion (equation 1 or 2) to determine which cracks, if any, may grow. In each cell, based on the stress, there is a critical size. In principle then, all cracks larger than the critical size grow at the asymptotic crack velocity for the duration of the cycle. Even for relatively simple stress histories, the critical crack size would have to be saved for each cell for each cycle. In the BCM, this problem is overcome by using a two parameter fit to represent the distribution function. Crack growth is not allowed until the critical size (c_{min}) reaches its minimum value. At this point, all cracks larger than this value of c_{min} are assumed to grow. The unstable cracks continue to grow until the smallest active cracks no longer satisfy the Griffith criterion. The time interval of active growth is one parameter and c_{min} is the second.

MESH EFFECTS

The finite size of a computational cell leads to two problems, both associated with numerical diffusion. First, there is the diffusion of fracture ahead of the wave. As a steep wave propagates through a cell, the cracks behind the peak cause a degradation of the effective elastic moduli of the material. Since there is only one set of moduli for the cell, the wave begins to propagate through partially fractured material, leading to too much attenuation. The problem can be characterized in terms of two time scales. One scale is physical, representing the time for the material to suffer significant reduction of the effective moduli. The second scale is numerical, the transit time of the wave through the cell, i.e., the cell size divided by a sound speed. When the numerical time scale becomes comparable to the physical time scale, numerical diffusion of the effects of fracture becomes significant.

The second problem is associated with the use of artificial viscosity to represent shock waves in the mesh (Wilkins, 1980). The artificial viscosity smears the numerical precursor to the shock over three or four computational cells. Because all cracks grow with the same asymptotic speed (Dunlavy and Brace, 1960), the shape of the precursor plays an important role in determining the amount of fracture ahead of the wave peak. The real rise time of the pulse is probably much less than is simulated with artificial viscosity.

In the BCM, we prevent fracture in the precursor by not allowing crack growth until the wave peak is detected. This corresponds to assuming a very sharp wave front, so it underestimates slightly the attenuation. This treatment reduces the effect of the first problem, the diffusion of fracture. When the cells are large the attenuation may be greatly underestimated.

The effect of fracture in one-dimensional wave propagation is to cause an exponential attenuation (Piau, 1979). However, the attenuation coefficient is sensitive to mesh spacing if the cells are too large. This is demonstrated in Fig. 1, where we plot the calculated attenuation coefficient, μ , against cell size for a one-dimensional problem. For small cells, the attenuation asymptotically approaches a constant value. The figure shows that a critical point occurs when $\mu\Delta x \approx 1$. This is consistent with the criterion for numerical diffusion since $(\mu c_s)^{-1}$ is a time for fracture and $(\Delta x/c_s)$ is the transit time of a cell. Here c_s is a sound speed. If it is not possible to use sufficiently small cells, a shock fitting technique that allows subgrid resolution of the wave must be employed.

APPLICATION TO OIL SHALE

The BCM has been used with the two-dimensional stress wave code, YAQUI, to simulate fracture of oil shale by high explosives.

YAQUI is a finite difference "ALE" (Arbitrary Lagrangian-Eulerian) code (Amsden, Ruppel, and Hirt 1980). The ALE formulation allows the oil shale to be followed in Lagrangian coordinates, preserving material interfaces, while the high explosive gases are followed in nearly Eulerian coordinates as they rush up the borehole past the oil shale.

The version of the BCM used for the calculations assumes that the penny shaped cracks all lie in planes parallel to the bedding planes. This is a reasonable first approximation, since the bedding planes in oil shale are planes of weakness (Youash, 1969). Reasonable values are assumed for the initial crack density and mean crack size. These quantities are measurable, in principle, in the laboratory, although studies at SRI (Murri et al., 1977) have shown that it is difficult to identify the pre-existing cracks and flaws in direct microscopic observations in oil shale. The elastic constants for the rock matrix in which the cracks are embedded are taken from published fits to laboratory data (Johnson, 1979).

The YAQUI code with the BCM constitutive model has been used to simulate a series of oil shale blasting experiments that was conducted in the Colony Mine near Parachute, CO. These experiments were done in cooperation with the Colony Development Corporation and Atlantic Richfield. Experiment 79.10 involved 24.7 kg of a commercial ammonium nitrate/fuel oil explosive (ANFO) emplaced in a 0.15 m-diameter borehole drilled vertically into the mine floor. The charge was 1.7 m in length and the depth to the bottom of the charge was 3.3 m. The charge was detonated from the bottom.

Experiment 79.10 produced a crater filled with loose rubble. The crater was subsequently excavated and profiles of the crater were measured for comparison with the calculations. The predicted fracture distribution 3.0 m-sec after the firing of the detonator is shown in Fig. 2. A typical measured cross section for the 79.10 crater is also shown in this figure. The predicted extent of fracture at the free surface agrees well with the width of the crater in the field. The code also predicts a large amount of fracture beneath the observed crater. However, the crater is not just the region where cracks have grown, but where complete fragmentation and tumbling of the rubble has occurred as well. Thus, we expect the observed crater to be shallower, since the broken rock at depth is locked in place and does not acquire upward momentum.

It is instructive to compare the predicted fracture for experiment 79.10 with the observed crater profile for experiment 79.12. That experiment consisted of four charges, each of which was approximately the same in size and depth of burial as the single charge in experiment 79.10. The four charges were arranged in a 3.2 m square pattern. A typical profile of the experiment 79.12 crater (along one side of the pattern) is shown in Fig. 3, along with the predicted fracture pattern, centered on one of the charges.

There is a good agreement between the predicted fracture and the observed crater from the surface down to about the level of the bottom of the charge. The effect of having four charges, spaced as in experiment 79.12, therefore appears not to be an increase in the extent of breakage, but rather in the total amount of loose and tumbled rubble. This probably has to do with the occurrence of multiple shocks and the way the high pressure explosive product gases penetrate into the shock-induced fracture network. The net effect is to cause the rubble-filled crater to more closely match the extent of the fractured rock. The calculation shows predicted fracture below the explosive borehole. This fractured rock will not be tumbled, even in a multiple borehole experiment, because of its location.

Code calculations can also be compared with field data from acceleration, velocity, and stress gauges. Measurements of peak vertical velocity at several locations on the free surface were made in a recent field experiment. That experiment was similar to experiment 79.10, except that low-density INT replaced ANFO as the explosive. The predicted and observed peak velocities are plotted against range from ground zero in Fig. 4. This figure shows good agreement between the calculations and the observations.

ACKNOWLEDGEMENTS

This work was supported by the U. S. Department of Energy, Office of the Assistant Secretary for Fossil Energy.

REFERENCES

- Amsden, A. A., Ruppel, H. M., and Hirt, C. W., 1980, "SALE: A Simplified ALE Computer Program for Fluid Flow at All Speeds," LA-8095, June, Los Alamos, NM, available from National Technical Information Service, Springfield, VA.
- Dunlaney, E. N., and Brace, W. F., 1960, "Velocity Behavior of a Growing Crack," Journal of Applied Physics, Vol. 31, No. 12, December, pp. 2233-2236.
- Griffith, A. A., 1920, "The Phenomena of Rupture and Flow in Solids," Philosophical Transactions of the Royal Society A, Vol. 221, No. 6, October, pp. 163-198.
- Hoenig, A., 1979, "Elastic Moduli of a Non-Randomly Cracked Body," International Journal of Solids and Structures, Vol. 15, No. 2, February, pp. 137-154.
- Johnson, J. N., 1979, "Calculation of Explosive Rock Breakage: Oil Shale," Proceedings of the 20th U. S. Symposium on Rock Mechanics, June, U. S. National Committee for Rock Mechanics, pp. 109-118.

- McClintock, F. A., and Walsh, J. B. 1962, "Friction on Griffith Cracks in Rocks Under Pressure," Proceedings of the 4th U. S. National Congress of Applied Mechanics, Berkeley, CA, pp. 1015-1021.
- Murri, W. J., et al., 1977, "Determination of Dynamic Fracture Parameters for Oil Shale, Final Report Covering the Period 1 June 1976 to 30 September 1976, Contract 03-4487 Under AT(29-1)-789," Stanford Research Institute, Menlo Park, CA, 42 pp.
- Piau, M., 1979, "Attenuation of a Plane Compressional Wave by a Random Distribution of Thin Circular Cracks," International Journal of Engineering Science, Vol. 17, No. 2, February, pp. 151-167.
- Shockey, et al., 1974, "Fragmentation of Rock Under Dynamic Loads," International Journal of Rock Mechanics and Mining Science and Geomechanics Abstracts, Vol. 11, No. 8, August, pp. 303-317.
- Wilkins, M. L., 1980, "Use of Artificial Viscosity in Multidimensional Fluid Dynamic Calculations," Journal of Computational Physics, Vol. 36, No. 2, July, pp. 281-303.
- Youash, Y., 1969, "Tension Tests on Layered Rocks," Geological Society of America Bulletin, Vol. 80, No. 2, February, pp. 303-306.

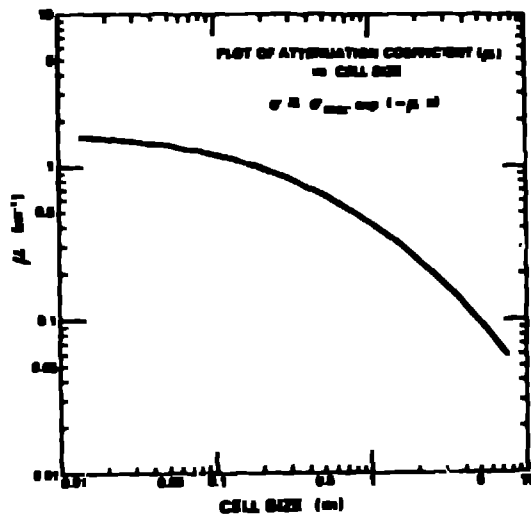


Fig. 1. Attenuation coefficient versus cell size.

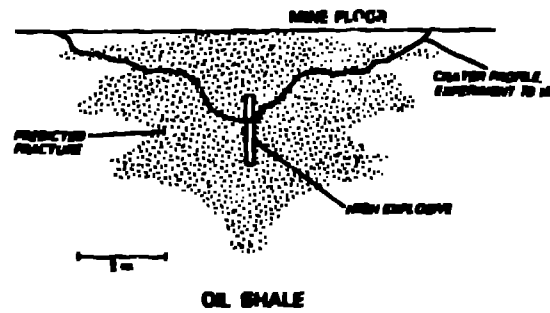


Fig. 2. Predicted fracture and observed crater for experiment 79.10.

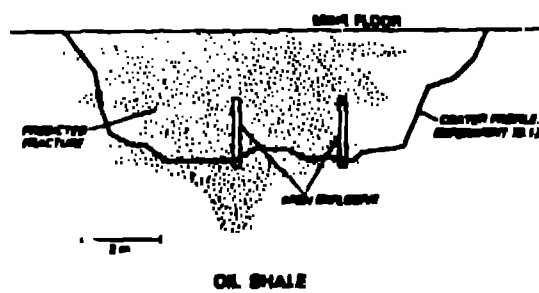


Fig. 3. Predicted fracture for experiment 79.10 and observed crater for experiment 79.12.

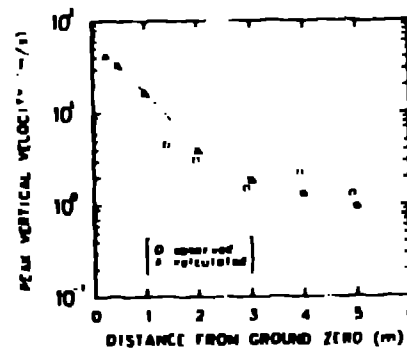


Fig. 4. Peak vertical velocity versus distance from ground zero.